SLAC–PUB–7339
November 1996

The Fabrication of Millimeter-Wavelength Accelerating Structures*

P.J. Chou, G.B. Bowden, M.R. Copeland, A. Farvid, R.E. Kirby, A. Menegat, C. Pearson, L. Shere, R.H. Siemann, J.E. Spencer and D.H. Whittum

Stanford Linear Accelerator Center
P.O. Box 4349, Stanford, CA 94309

Abstract

There is a growing interest in the development of high gradient (≥ 1GeV/m) accelerating structures. The need for high gradient acceleration based on current microwave technology requires the structures to be operated in the millimeter wavelength. Fabrication of accelerating structures at millimeter scale with sub-micron tolerances poses great challenges. The accelerating structures impose strict requirements on surface smoothness and finish to suppress field emission and multipactor effects. Various fabrication techniques based on conventional machining and micromachining have been evaluated and tested. These will be discussed and measurement results presented.

An abridged version was contributed to *the 7th Workshop of Advanced Accelerator Concepts*

Lake Tahoe, California, October 12- 18, 1996

* Work supported by Department of Energy contract DE–AC03–76SF00515.

1. INTRODUCTION

High gradient acceleration based on current microwave technology requires the structure to be operated at higher frequencies in order to reduce power consumption[1]. To determine the limit of particle acceleration based on microwave technology, a millimeter wavelength is chosen. According to frequency scaling[2, 3], the dimensional tolerance required for mm-wave structures ranges from 2 μm to 0.6 μm. The fabrication of accelerating structures at the millimeter scale with sub-micron tolerances poses great challenges. Accelerating structures at millimeter scale are quite small for conventional machining. Another option is to fabricate them by using micromachining techniques such as LIGA[4]. The operating frequency for the test structure is tentatively chosen to be around 32 times SLAC frequency (32 × 2.856 GHz). Accelerating structures at this scale are too big for most micromachining techniques. The suppression of field emission and multipactor effects places strict requirements on surface roughness and finish. Post machining surface treatment is also important.

The muffin-tin structure[4] is used because it is relatively easy to fabricate by micromachining compared to a cylindrical structure. The schematic sketch of a 6-cell structure is depicted in Fig. 1. Physical dimensions of the muffin-tin slab and two sidewalls are given in Fig. 2.

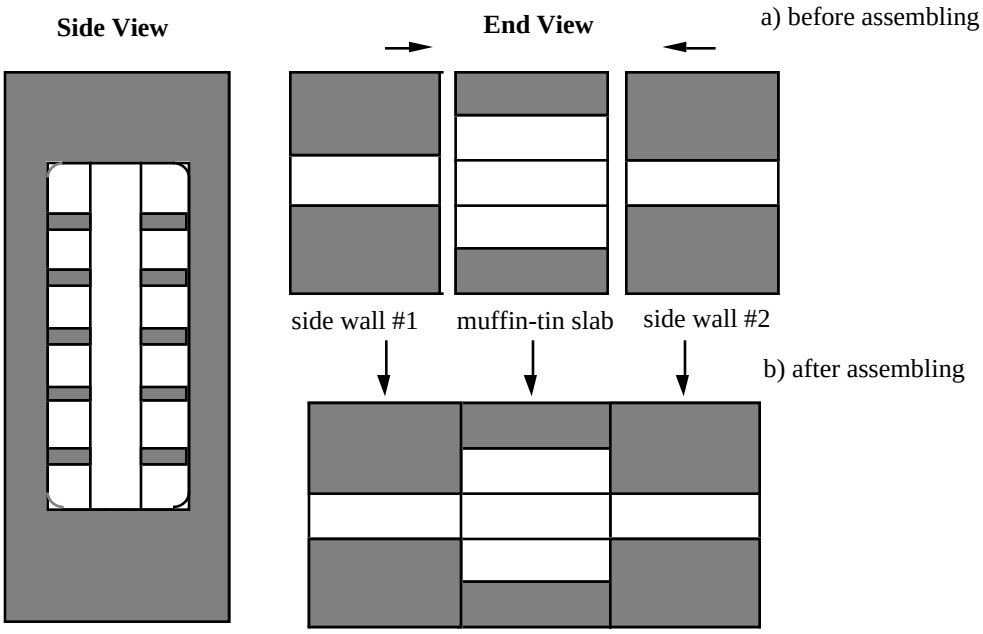

Fig. 1: The schematic sketch of the muffin-tin accelerating structure.

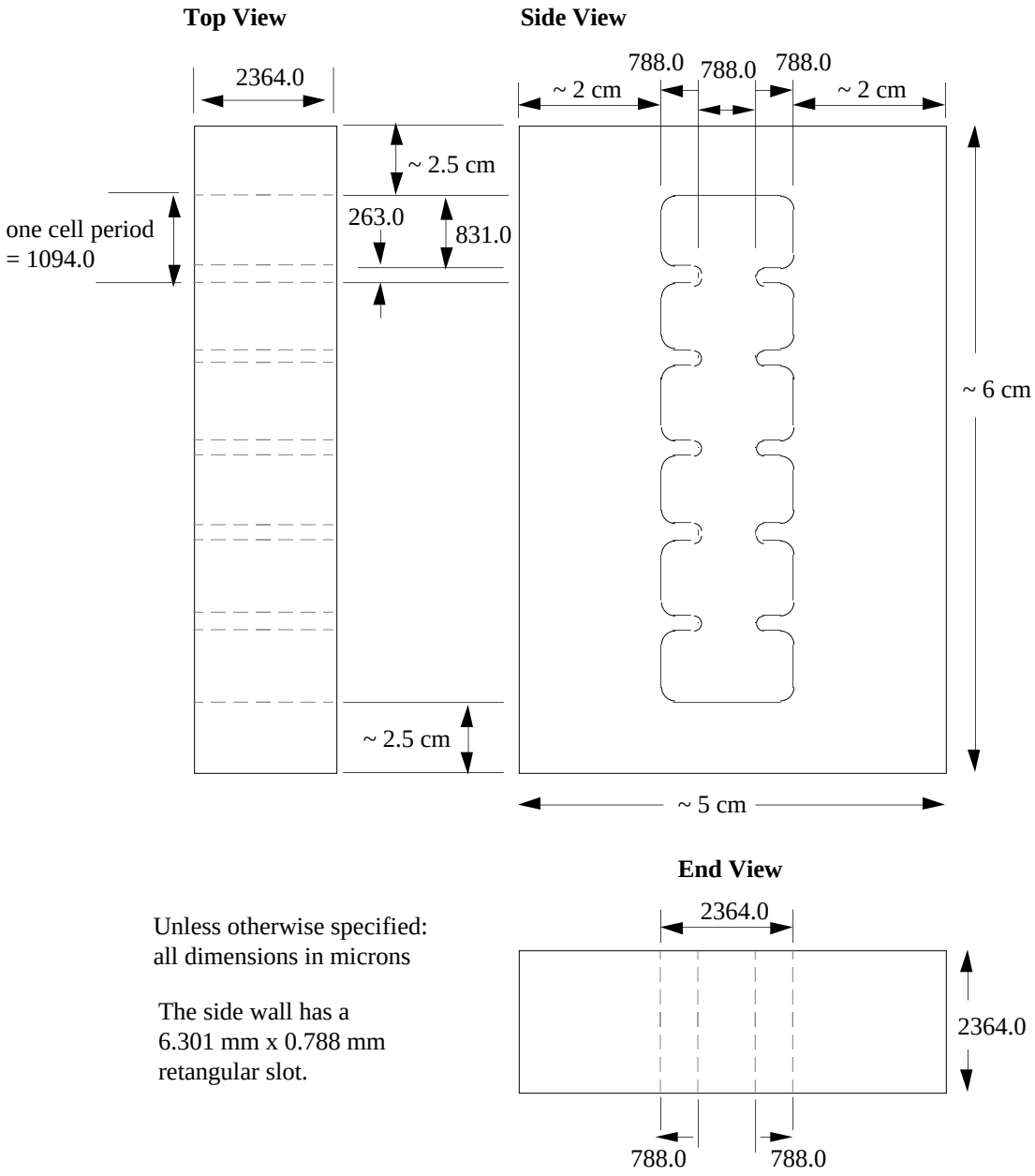

Fig. 2: Physical dimensions of muffin-tin slab.

Consider a surface profile at the microscopic scale depicted in Fig. 3. The quantity R_a used to characterize the surface roughness is defined below[5]:

$$R_a = \frac{1}{n}\sum_{i=1}^{n}|z_i|$$

where n is the total number of measurements and z_i is the profile amplitude of surface. This definition does not consider cases where average surfaces are tilted or offset with respect to the x axis. R_a is the arithmetic average of the absolute values of all profile amplitudes z_i within the entire measurement range. It should be noted that R_a is just one of several quantities used in surface metrology to characterize a surface profile. It may not be the best way for certain applications.

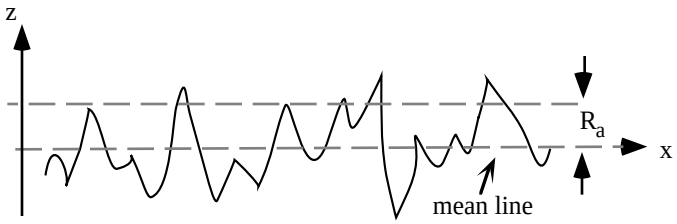

Fig. 3: The microscopic view of surface profile.

2. PRECISION MACHINING

I. Wilson gave a thorough review on the fabrication of RF cavities based on conventional machining techniques[6]. Conventional machining techniques are suitable for making large accelerating structures at the scale of a few tens of centimeters or bigger. For mm-wave structures, one also needs to consider micromachining techniques.

2.1. Laser machining

Laser pulses can be used to cut metal with good accuracy. The current dimensional tolerance quoted for this technique is ± 0.0001" (2.5 μm). This is not adequate for mm-wave structures. Too, this technique has other drawbacks. The cutting process will cause burrs and produce a rough surface finish (class 125 or $R_a \approx$ 3.2 μm). It is not a suitable process for copper because of the poor edge definition and 1 mm thick copper sheet is too thick for laser machining. Even for copper sheet of 500 μm, the above problems still exist.

2.2 Hydraulic cutting

A highly pressurized water jet mixed with abrasive particles is used to cut metal. This is an abrasive process and produces rough surface finish. The size of water jet is not small enough to cut small features on the workpiece. Therefore, it is not suitable for the fabrication of mm-wave structures.

2.3 Single-point diamond turning[5]

A cutting tool with a small diamond tip can be used to machine non-ferrous materials such as aluminum and copper to obtain a very fine surface finish. The cutting process is illustrated in Fig. 4. Single-point diamond turning is usually carried out at a turning speed of 2500- 5000 rpm. Typical roughness for ordinary diamond turning may be around 25-50 nm or better.

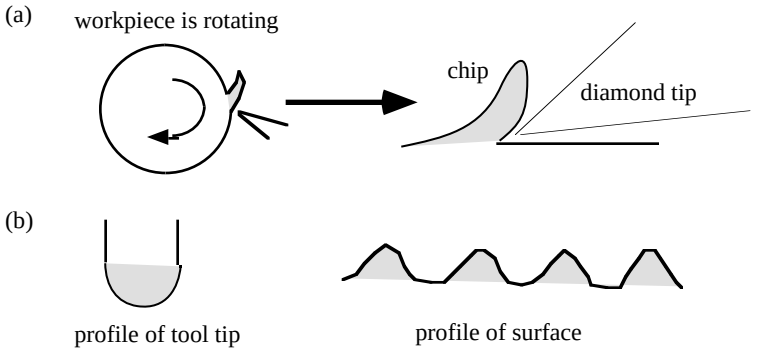

Fig. 4: The single-point diamond machining process

Compared with conventional cutting, the influence of anisotropy of the material on surface roughness can not be neglected. Single-point diamond turning is best suited to cut axi-symmetric geometry such as mirrors or lenses. For mm-wave structures with complicated 3D geometry, this technique may not be suitable.

One drawback of single-point diamond turning is burrs left along part edges or whenever there is an interrupted cut as depicted in Figs. 5 and 6. These burrs are quite pronounced. Sharp points are likely to become field emitters under high power operation. Further surface treatment may be necessary in order to remove burrs.

Because of the concern for surface damage from pulse heating[7, 8], a dispersion strengthened copper called glidcop® might be a better choice as the base material than pure copper. Unfortunately single-point diamond turning does not work well with glidcop®. The cutting tool could be damaged by the alumina particles present in the glidcop®[9].

Single-point diamond turning will also leave machining marks on the surface. The transverse profile of these marks is illustrated in Fig. 4. They will not be an exact replica of the cutting tool, partly because of the burnishing effect of the cutting tool. Machining marks left by the cutting tool are clearly shown in Fig. 7. The corresponding 3-dimensional surface profile is depicted in Fig. 8. The surface roughness R_a is 0.018 μm.

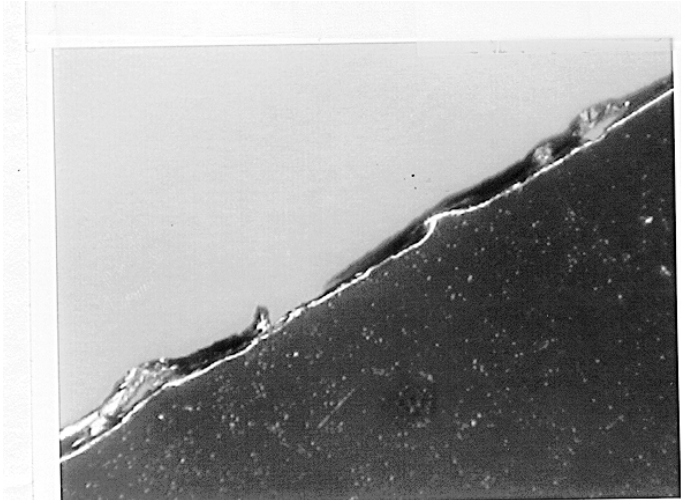

Fig. 5: Burrs left along cutting edges in single-point diamond turning. Picture was taken by optical microscope for a NLC test structure[3].

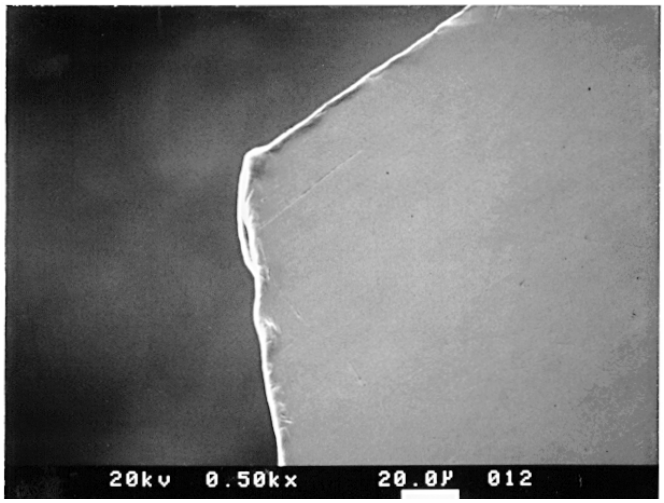

Fig. 6: Burrs left along cutting edges in single-point diamond turning. Picture was taken by scanning electron microscope. The white bar represents 20 μm.

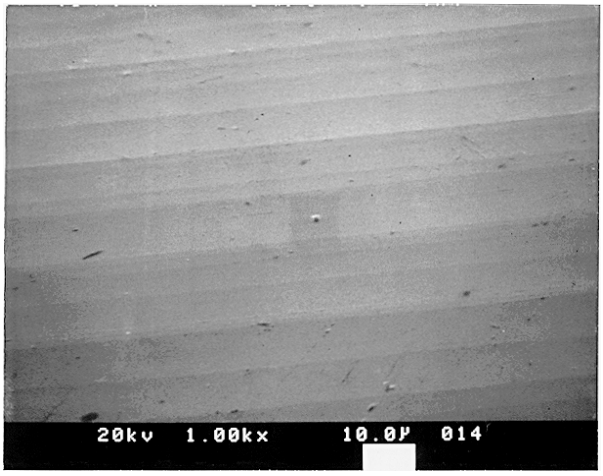

Fig. 7: Machining marks left by the cutting tool in single-point diamond turning. The bar represents 10 µm. From one of NLC test structures. Picture was taken by a scanning electron microscope.

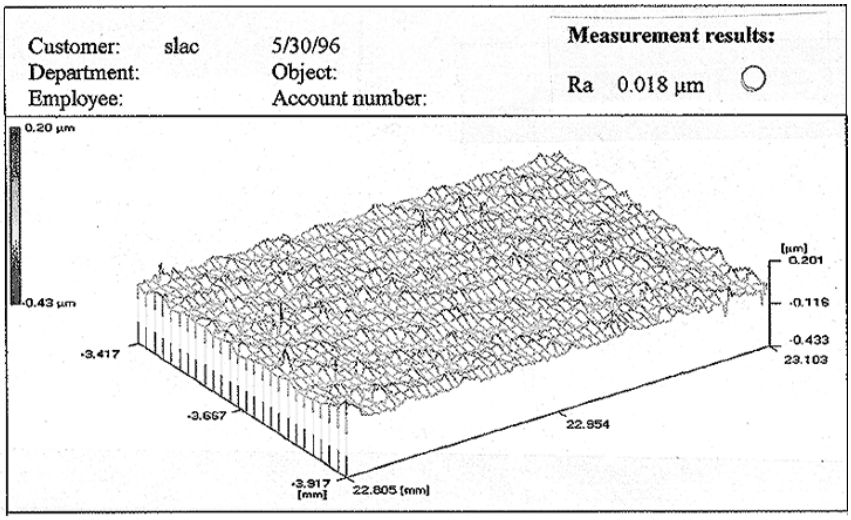

Fig. 8: Three-dimensional surface profile of single-point diamond machined NLC test structure[10].

2.4 Photochemical machining[11, 12]

This technique is suitable for precision machining of thin metal sheets. It offers burr free edges. The machining process is illustrated in Fig. 9. The design feature is generated on a photomask by using laser plot technology[11]. A thin layer of photosensitive, etchant-resistant polymer called photoresist is coated onto both sides of metal surface. Then the photoresist is exposed and developed. The

metal surface is selectively masked by the photoresist. Therefore, the design feature is transferred from the mask to the photoresist. Heated etching solution (acid) is sprayed on both sides of metal. Those regions which are not covered by the photoresist will be etched away. Then the photoresist is removed. When the etching solution impinges on the metal surface, some erosion on the side wall also occurs. This side erosion called undercut is indicated in step five of Fig. 9. This is the main factor governing the tolerances that can be held. As the thickness of metal sheet increases, so does the undercut. The tolerances that can be held also increase accordingly. As a general rule of thumb, the minimum feature size can not be less than the thickness of metal sheets used for machining. Typical planar dimensional tolerances are ± 0.0005" within 6" range[12].

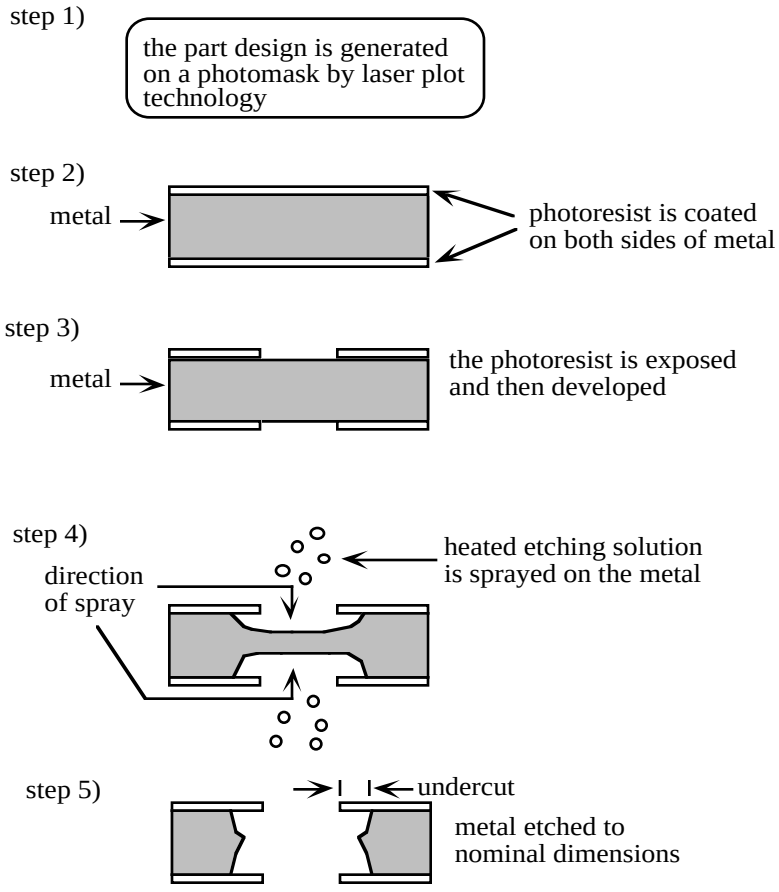

Fig. 9: The photochemical machining process.

This technique allows intricate geometries to be made on metal sheets. It is also an inexpensive approach for mass production. In order to achieve tight tolerances required for mm-wave structures, the thickness of metal sheets should not be larger than 0.01" for critical dimensions. Cylindrical structures with high

order mode damping slots, pumping ports, input and output couplers can be fabricated into a single piece at the same time. That would require the structure to be built from laminations and probably bonded by diffusion bonding. The flatness of metal sheets and the accuracy of assembling within one micron then become important issues. At this moment, answers to those questions are not clear. Figure 10 depicts the intricate geometries fabricated by photochemical machining. Surface treatments are required to insure a smooth surface for bonding.

Fig. 10: A stainless steel sheet with intricate geometriey made by photochemical machining[11]. The physical dimension of the view area is roughly 2"× 2". Picture was taken by an optical microscope.

2.5 Precision diamond grinding[5, 13]

Grinding wheels are made up of a large number of abrasive grains held in a bonding agent. The abrasive grain can be aluminum oxide, silicon carbide, cubic boron nitride or diamond. The process is illustrated in Fig. 11. The grinding wheel is first formed to the design shape by a dressing tool. Then the rotating grinding wheel is brought to the workpiece to remove metal. The surface roughness has to do with wheel characteristics, e.g. the grain type, grain spacing, grain size, dressing method, wheel balance ... etc. Precision diamond grinders with 0.00001" programmable step are available from commercial companies. Dimensional tolerances are often down to ±0.00005" (± 1.3 μm), and to a 0.000003" surface finish (R_a= 0.08 μm). The drawback of this technique is grain inclusion on the metal surface. The grains can not be removed easily by surface polishing treatments. Since they could become field emitters under high power operation, this is a fatal drawback of the use of grinding techniques for the structure fabrication.

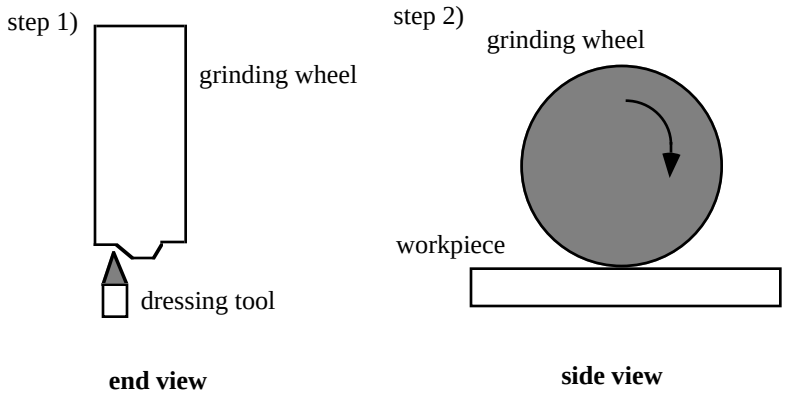

Fig. 11: The process of grinding.

2.6 Electrodischarge machining (EDM)[5, 14]

This method can be used to machine very hard materials. The process is illustrated in Fig. 12.

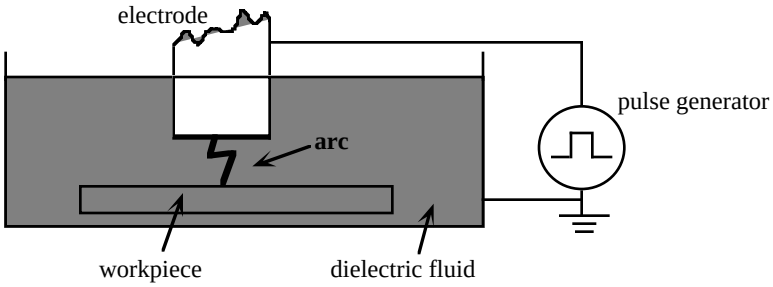

Fig. 12: The basic setup for electrodischarge machining process.

The machining tool (electrode) is placed about 25- 50 μm away from the workpiece. The tool electrode is connected to a pulsed voltage source. If the potential difference between the tool and workpiece is high enough, a spark is produced and the dielectric fluid ionized. The dielectric fluid is usually oil or water. If the potential difference is maintained, the spark will developed into an arc which causes the removal of metal. If the potential difference falls the arc decays. The temperature of the arc is the property responsible for removing metal. Typical values are between 5000 and 10000 ^{o}C; well above the melting point of most metals. The tool electrode is made of conducting materials, such as copper. For long life and high form accuracy, tungsten carbide is sometimes used. The surface of EDM'ed workpiece looks like shot blasting. There are many craters on the

surface, also known as pits in EDM terminology. Figure 13 depicts a typical result of EDM'ed copper surface.

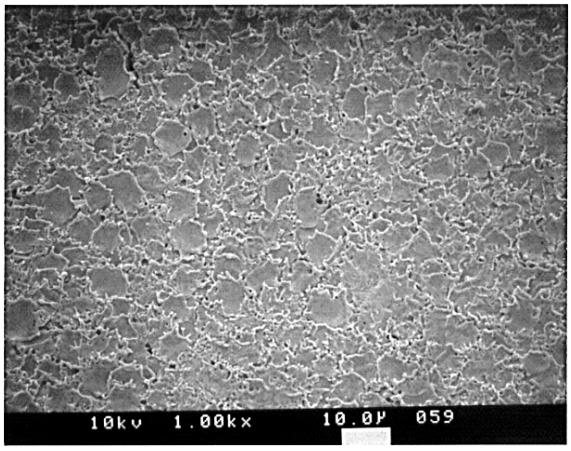

Fig. 13: The surface finish of oxygen free copper cut by electrodischarge machining. Picture was taken by scanning electron microscope. Picture was taken by a scanning electron microscope.

A wire EDM machine uses a continuously spooling conducting wire as electrode which moves in prescribed patterns around the workpiece. The typical tolerances can be down to 3-5 μm. A new generation of wire EDM machines began to emerge a couple of years ago. Machine manufacturers claim that a sub-micron accuracy can be achieved. Currently this possibility is being explored. Figure 14 depicts a typical setup of wire EDM. A 3D surface profile of oxygen-free copper machined by wire EDM is shown in Fig. 15. The surface finish produced by wire EDM is inferior to single-point diamond turning. Further surface treatments are definitely needed.

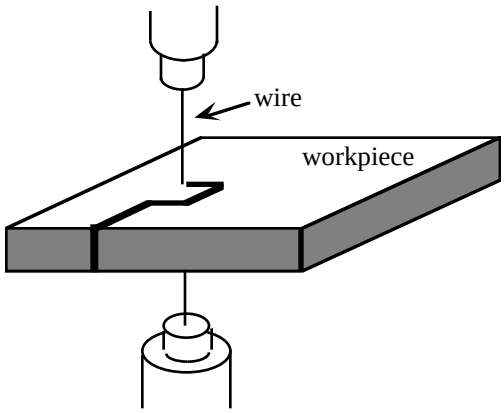

Fig. 14: A typical setup of wire electrodischarge machining.

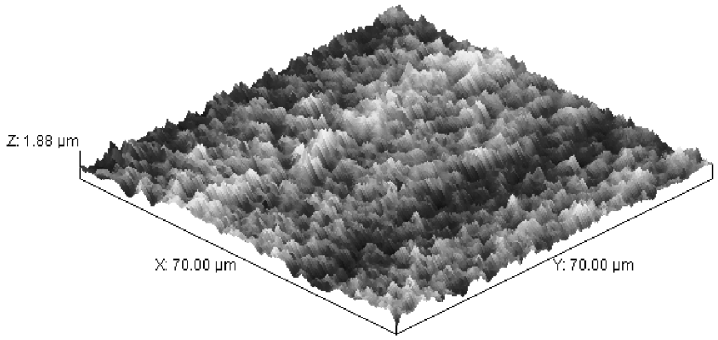

Fig. 15: The 3D surface profile of oxygen-free copper machined by wire EDM, $R_a \approx 0.5$ µm[10]. Picture was taken by atomic force microscope.

Test parts for muffin-tin structures operating around 92 GHz and 11 GHz have been fabricated by wire EDM. Note that the current SLAC operating frequency is 2.856 GHz. Figures 16 and 17 depict the 92 GHz muffin-tin slab and the close-up view of a cavity iris prior to surface polishing respectively.

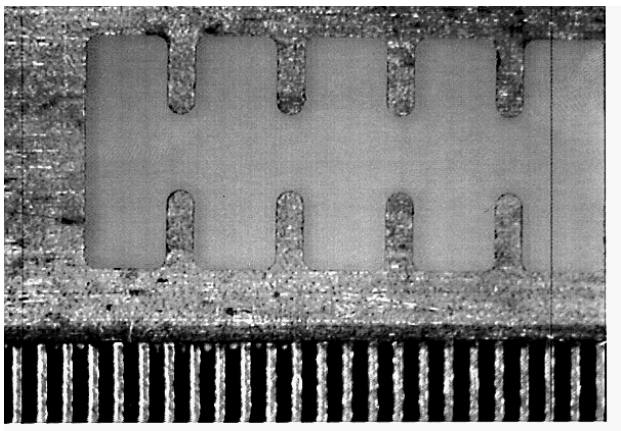

Fig. 16: A 92 GHz muffin-tin slab fabricated by wire EDM and aligned along a ruler. Each horizontal division is 0.01". Picture was taken by optical microscope.

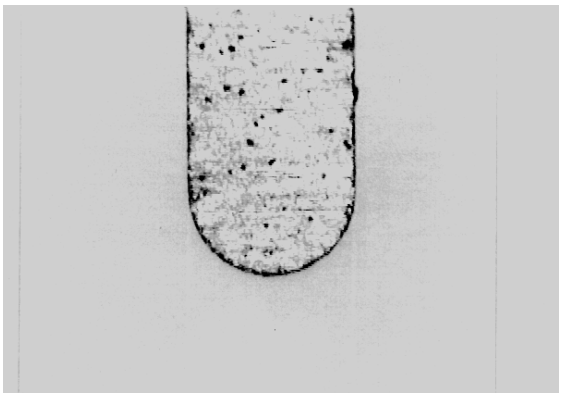

Fig. 17: The close-up view of a cavity iris in the 92 GHz muffin-tin slab. Picture was taken by optical microscope.

Closer examinations on areas depicted below for an 11 GHz muffin-tin slab are depicted in Figs. 18, 19 and 20.

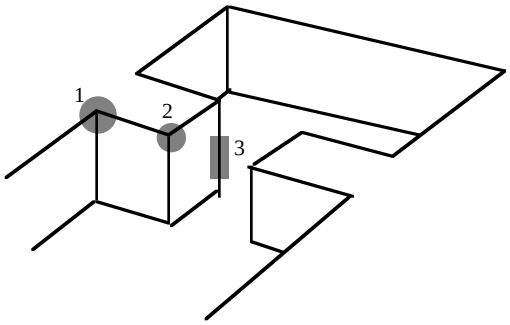

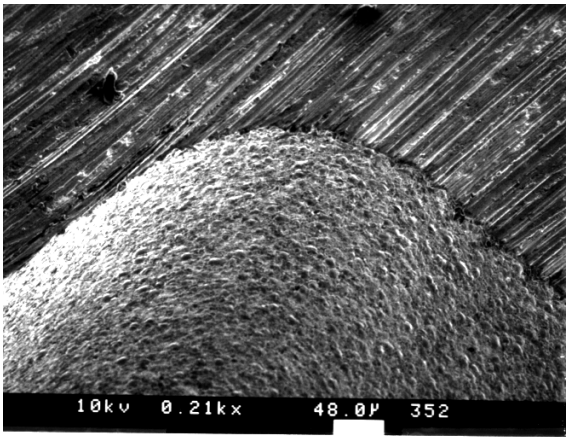

Fig. 18: Corner edge at the bottom of a cavity cell (region 1). Picture was taken by a scanning electron microscope.

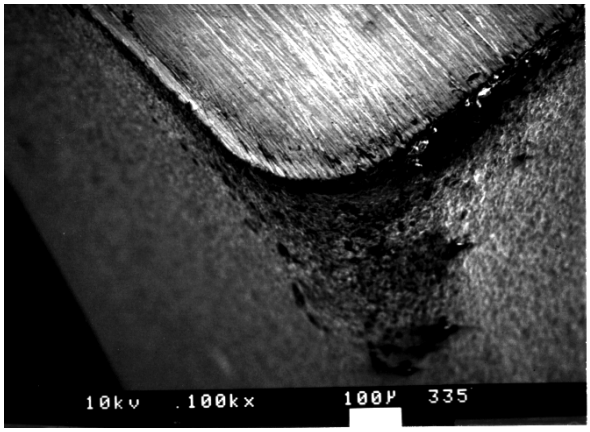

Fig. 19: Corner edge at the tip of a cavity iris (region 2).

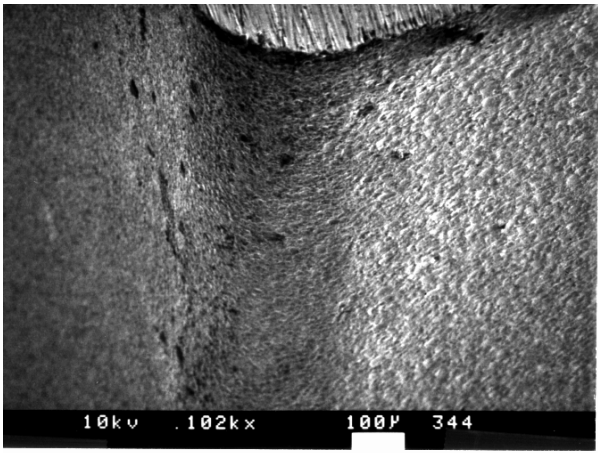

Fig. 20: Side edge along a cavity iris (region 3).

2.7 Precision electroforming[15, 16]

Electroforming is a process for fabricating a metal part by electrodeposition in a plating bath over a base form or mandrel which is subsequently removed. The advantage of this process is that it faithfully reproduces the form to within one micron[17]. The setup for electroforming is illustrated in Fig. 21.

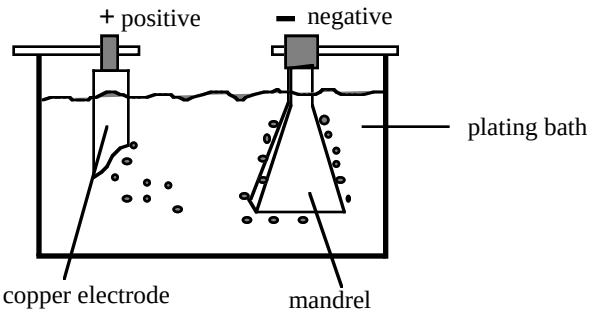

Fig. 21: Basic setup for electroforming process.

The dimensional tolerances of electroformed metal parts are determined by the accuracy of mandrels. Mandrels are prepared by machining techniques with tolerances of ± 0.0002"[17]. Therefore, electroforming can not provide adequate accuracy for mm-wave accelerating structures.

3. MICROMACHINING

Another possibility for fabricating mm-wave accelerating structures is micromachining. For industrial applications machining is normally used to fabricate parts with a size ranging from few millimeters to centimeters and dimensional tolerances ≥ 5 μm. In contrast, micromachining is normally used to fabricate parts with a size ranging from few tens to few hundreds of microns and dimensional tolerances around 5 μm, such as microsensors. Several micromachining techniques have been evaluated and summaries are presented below.

3.1 Optical lithography and wet chemical etching[18]

Optical lithography is an established method and extensively used by the IC industry. The vast majority of lithographic equipment for IC fabrication is optical equipment using ultraviolet (UV) light ($\lambda \approx$ 0.2 to 0.4 μm). An illustration of the basic process is depicted in Fig. 22. The wet chemical etching is an isotropic process which results in side erosion of the silicon substrate. Optical lithography can also be used to pattern very thick photoresist for the fabrication of microsystems. After the pattern is developed on the thick photoresist, microstructures are made by electroplating. So far the application of optical lithography has been restricted to a resist thickness up to 10 μm due to the limited depth of focus and diffraction[19]. Although patterning of resist layers up to 200 μm using UV light and contact printing was reported[20], it is still not adequate for making mm-wave structures which requires a thickness up to 2 mm.

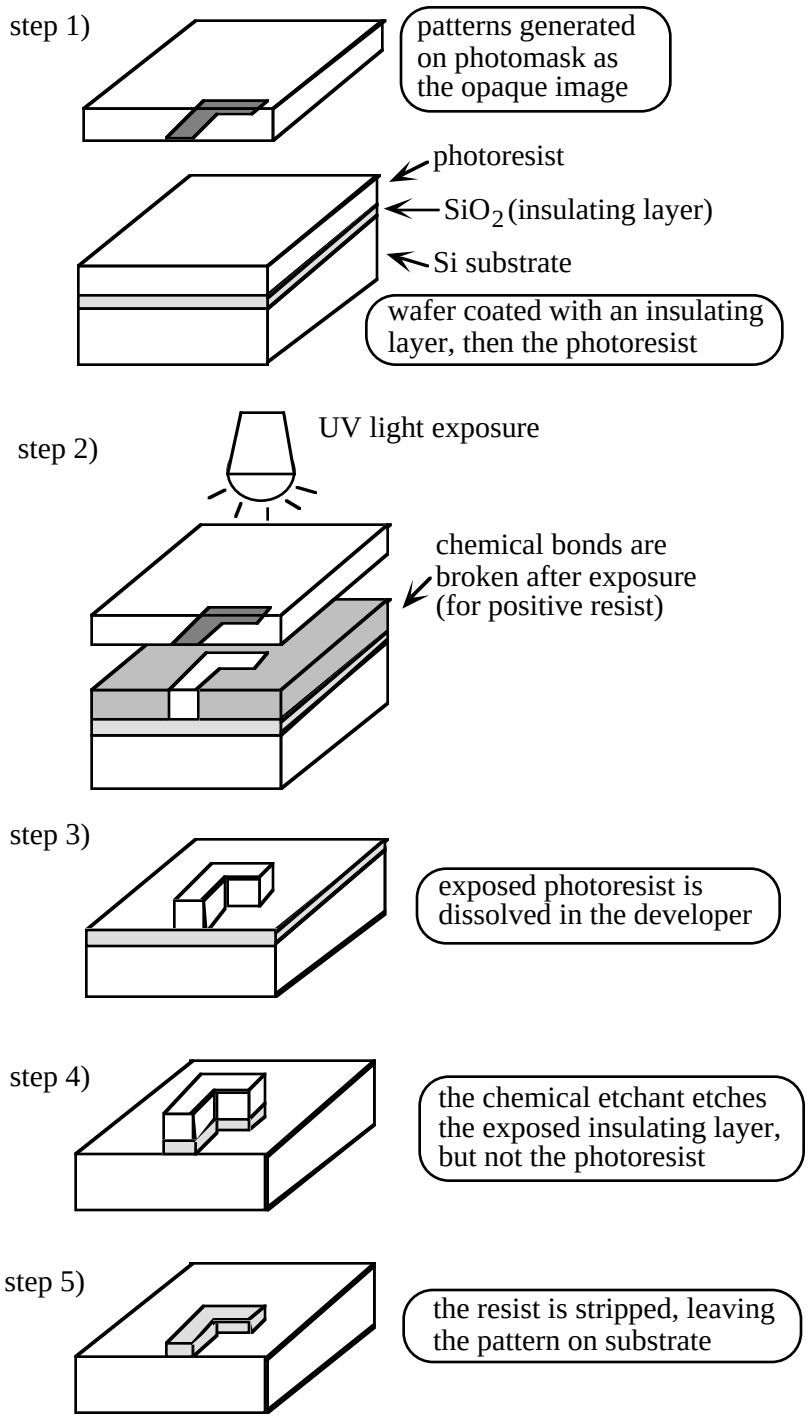

Fig. 22: The basic process of optical lithography with wet chemical etching.

3.2 Ion beam etching[18, 21]

The basic procedures are quite similar to optical lithography. The pattern is first developed on the photoresist layer, then an ion beam is used to etch the wafer material instead of wet chemicals. The setup is depicted in Fig. 23. This is a dry etching process. No chemical solution is used as the etchant. Noble gas is used to produce an ion beam for the etching.

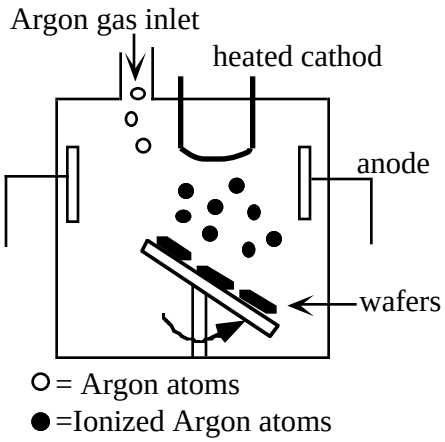

Fig. 23: Schematic of ion beam etching.

Typically, argon gas is introduced into the chamber. Upon entering the chamber, the argon is subjected to a stream of energetic electrons between cathode and anode electrodes. The argon atoms are ionized by the electrons into positively charged ions. Wafers are held on a negatively grounded holder which attracts the ionized argon atoms. As argon ions travel toward the wafers, they are accelerated and gain energy. When argon ions impinge on the exposed wafer surface, they literally knock out the atoms on the surface. This is a physical etching process. The etching mechanism is momentum transfer. No chemical reaction takes place between the argon ions and the wafer material. Ion beam etching is also called sputter etching or ion milling. The material removal is highly directional, resulting in good definition on small openings and high spatial resolution. Ion beam etching has very high resolution (about 100 Å) and is suitable for making sub-micron-range structures. Ion beam etching has poor selectivity on material, which means the etching rate is about the same for most materials. For copper the etching rate is 880 Å/min[22]. Silicon wafer of thickness up to 300 μm has been etched successfully by ion beam etching to produce design patterns[23]. At present it is unclear whether ion beam etching is suitable for making mm-wave structures or not.

3.3 Reactive-ion etching[18, 21, 24, 25, 26]

This is a combination of physical and chemical etching processes. The basic apparatus for reactive-ion etching (RIE) is depicted in Fig. 24.

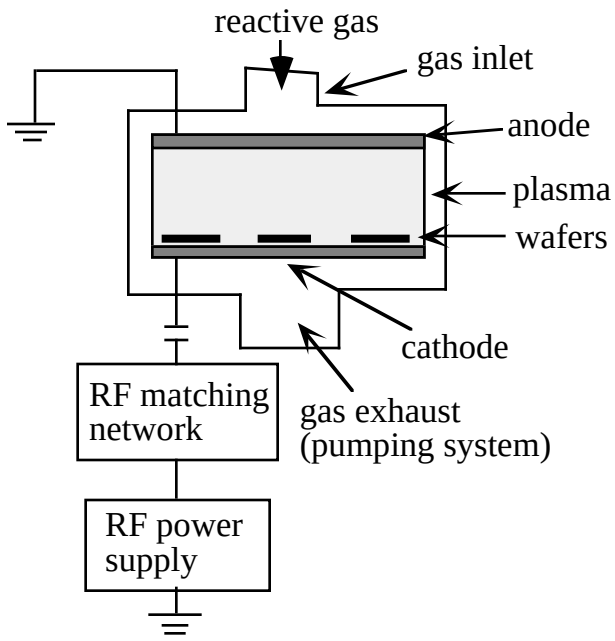

Fig. 24: The schematic sketch of an RIE etch chamber.

The reactive ions generated in the plasma are extracted and accelerated towards wafers. When the reaction between the reactive ions and surface material produces volatile compounds, etching occurs. Those volatile products are subsequently removed by vacuum pump. The ion bombardment helps to make the etching directional which results in almost straight sidewalls (high degree of anisotropy). Different gas composition will affect the selectivity or etch rate. An illustration of the etching process is given in Fig. 25. RIE is a highly selective process. For example, using gas mixture of BCl_3 and Cl_2 , the relative ratio of etch rate on Al to etch rate on SiO_2 is 25[18]. Using RIE to fabricate microelectrical mechanical systems has been reported for thickness up to few tens of microns[27]. Little work has been done on etching pure copper. Much work needs to be done in order to decide whether RIE is suitable for the fabrication of mm-wave accelerating structures.

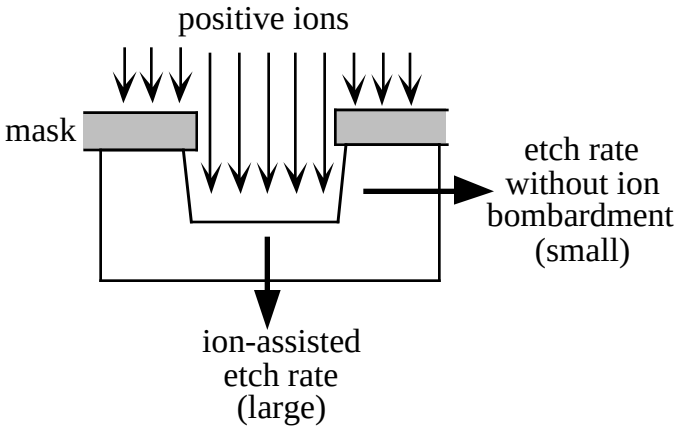

Fig. 25: The ion-assisted etching process.

3.4 Wet-chemical anisotropic etching of monocrystalline silicon[18, 28]

This technique is a variant of optical lithography with isotropic wet etching. Some chemical etchants dissolve a given crystal plane of a semiconductor much faster than other planes; this results in orientation-dependent etching. Using orientation-dependent etching one can attain V-shaped grooves or straight-walled grooves. Figure 26 depicts the orientation-dependent etching on certain monocrystalline silicon substrates. This technique provides a high degree of anisotropy and selectivity. It is suitable for making micromechanical structures. Micromechanical structures with depths up to 2 mm and dimensional tolerances of 0.0001" can be fabricated[28]. Accelerating structures made by anisotropic etching of silicon with tolerances of 5 μm have been reported[29]. After the silicon substrate is etched, copper is sputtered on to build a metallic layer. Because of pulse heating effects, the copper layer on the silicon substrate may not be able to sustain the fatigue damage. More knowledge from high-power pulse heating experiments is needed to determine whether or not this is a viable candidate for structure fabrication.

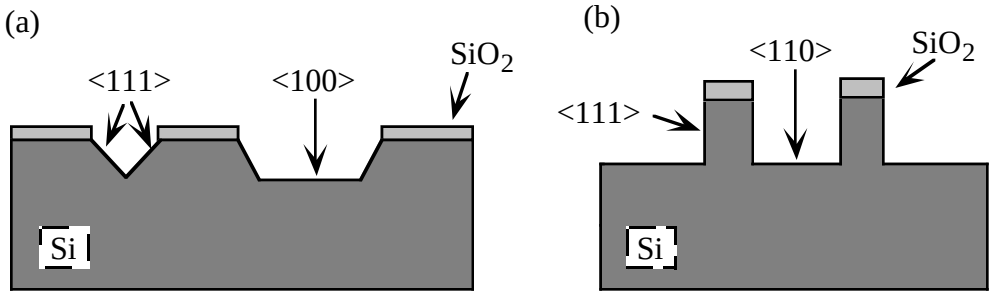

Fig. 26: Orientation-dependent etching (a) through window on <100>-oriented silicon (b) through window patterns on <110>-oriented silicon[18].

3.5 LIGA[30]

LIGA is a German acronym which stands for Lithogrphie, Galvanoformung, and Abformung. This is a combination of deep-etch X-ray lithography, electroforming and plastic molding processes. This is a technique for fabricating microstructures with extreme structural heights. The procedures for pattern generation on the resist layer are depicted in Fig. 27. The resist material is poly(methylmethacrylate) (PMMA). For producing metallic microstructures, the resist structure is generated on an electrically conductive substrate and metal is deposited from a suitable electrolyte as depicted in Fig. 28. A complementary metallic microstructure is obtained after electroplating which may be the final product or a mold insert for a subsequent replication. For mass production the electroformed structure is used as the mold insert. Many mandrels can be made from plastic by injection molding using thermoplastic materials. Then the microstructures are made by electroplating on those mandrels.

LIGA is an attractive option for fabricating mm-wave accelerating structures. It can provide approximately 2 μm true dimensional tolerances[31]. It is also suitable for mass production of structures. Unfortunately it requires a synchrotron light source to provide the highly collimated X-rays. The preparation of X-ray masks is also more complicated than masks used for optical lithography. At present LIGA remains as an expensive approach for fabricating mm-wave accelerating structures.

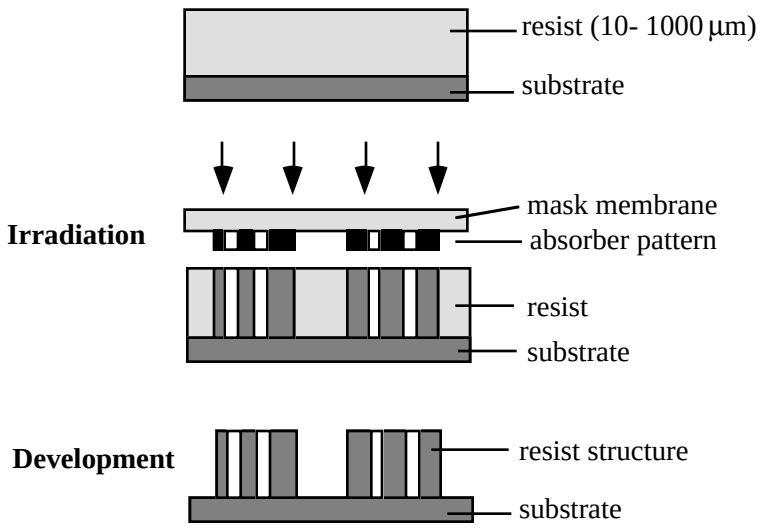

Fig. 27: Generation of resist pattern by deep-etch X-ray lithography[30].

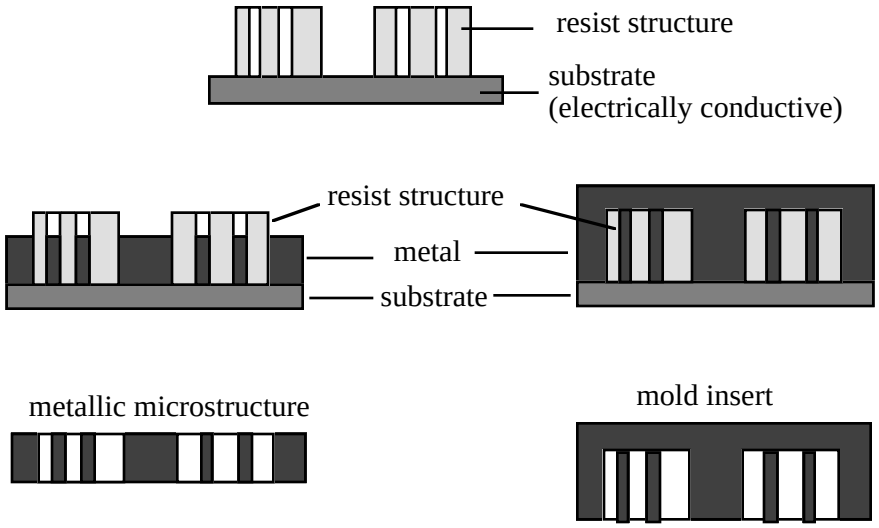

Fig. 28: Generation of a metallic microstructure and a mold insert respectively[30].

4. SURFACE TREATMENT— ELECTROPOLISHING[16, 32, 33, 34]

To prepare smooth surfaces for mm-wave accelerating structures, both chemical cleaning and electropolishing have been investigated. Because of the grain inclusion, mechanical polishing is not being considered. Experimental results show that electropolishing can remove high spots on the surface and incorporated electrode material from EDM.[35]. Because we had more success with electropolishing than chemical cleaning at SLAC, most of the work has been devoted to electropolishing with copper and results are presented below.

The apparatus for electropolishing is depicted in Fig. 29. Electropolishing is an electrochemical process, requiring an electrolyte and DC current. It is similar to electroplating but is the reverse. Acidic chemical solutions are used as the electrolyte and DC current is applied simultaneously. Metal is selectively removed from the surface under controlled conditions. With the application of current, high points of surface roughness and burr areas are higher current density areas than the rest of surface and are dissolved away at a greater rate. This results in smoothing, leveling and deburring. During the process hydrogen is liberated from the cathode and oxygen from the anode. The electropolishing operation requires the proper balance between voltage and current. If the current density is too high, both the valleys and the peaks on the metal surface will be etched, resulting in pitting and gas evolution. When the current density is too low, etching occurs, resulting in non-specific removal of metal. The smoothness of electropolished surface is also dependent on the surface finish prior to the operation. An ideal relationship between current density and voltage is represented in Fig. 30. The key factors which affect the final surface finish are temperature, composition of chemical solutions, voltage, time and solution agitation.

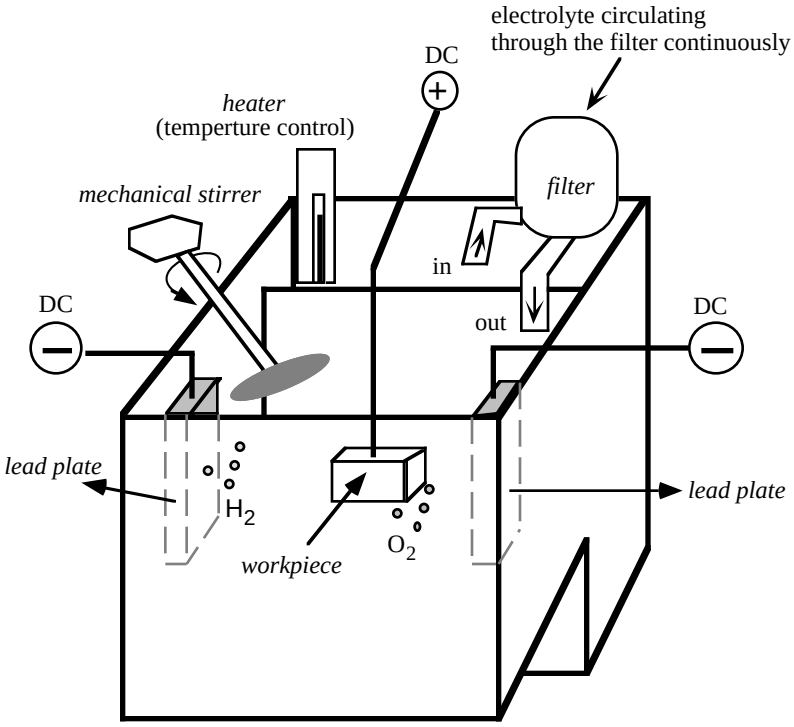

Fig. 29: The apparatus used in electropolishing operation.

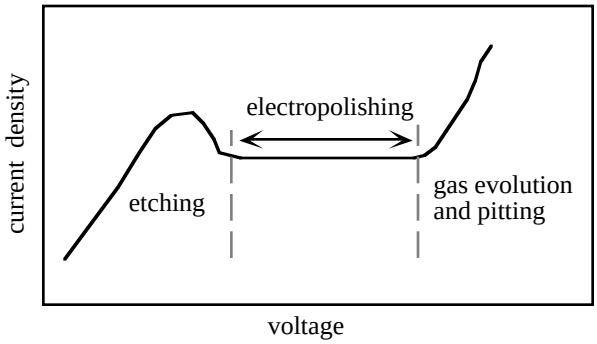

Fig. 30: Ideal relationship between current density and voltage in electropolishing cell.

Figure 31 depicts the surface finish of copper cut by wire EDM and treated by electropolishing without agitation for 4 minutes. The copper removal rate is about 1 μm per minute. Comparing with Fig. 15, high points on the surface are smoothed out and the roughness is reduced by about a factor of 3 ($R_a \approx 0.2$ μm). After the electropolishing the grain boundary of pure copper can be seen clearly as depicted in Figs. 32 and 33.

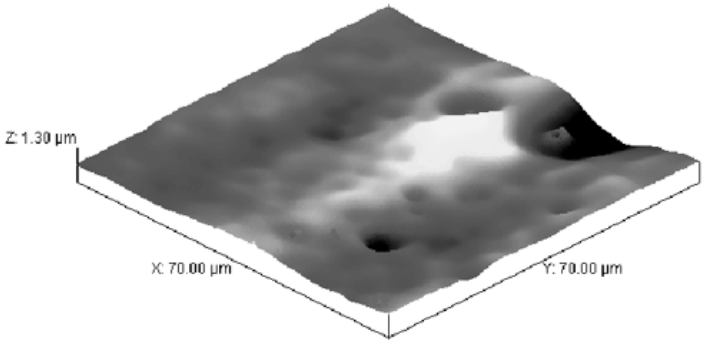

Fig. 31: Surface finish of copper cut by wire EDM and treated by electropolishing for 4 minutes. Picture was taken by an atomic force microscope.

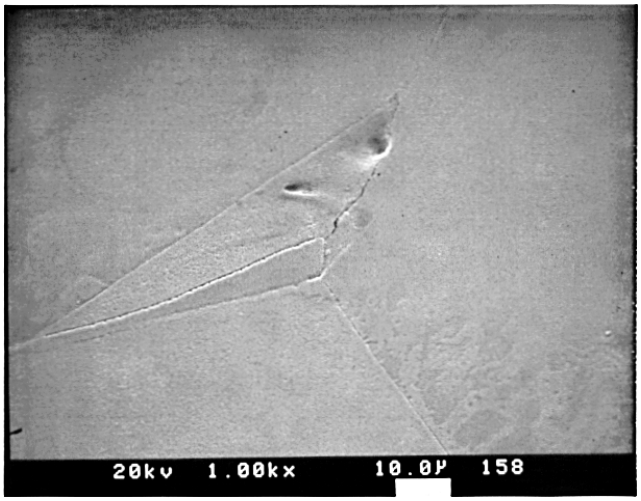

Fig. 32: The surface of copper cut by wire EDM and treated by electropolishing. The white bar represents a length of 10 µm. The crystal grains of pure copper can be seen clearly. Picture was taken by a scanning electron microscope.

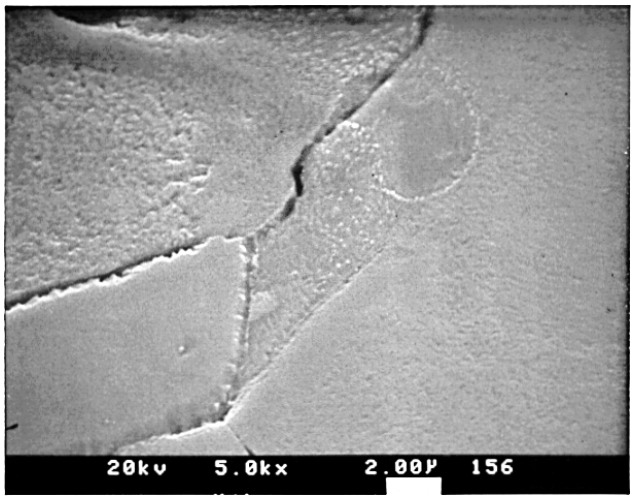

Fig. 33: A close-up view of the grain boundary for pure copper. Picture was taken by a scanning electron microscope.

When there is no agitation introduced to the bath, the surface waviness begins to develop as the processing time is increased. The surface waviness is depicted in Fig. 34; the processing time is 8 minutes.

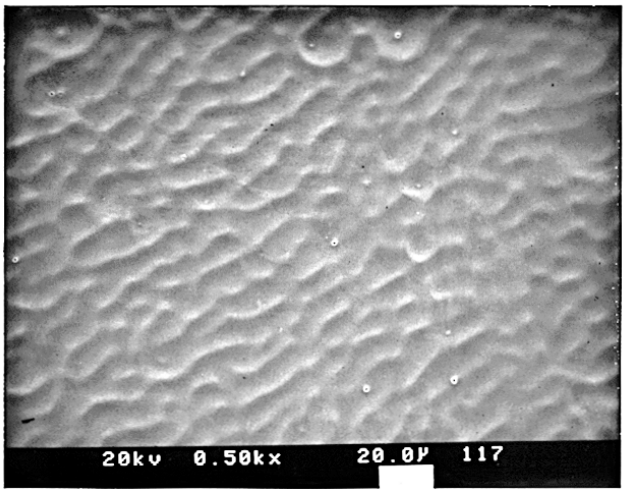

Fig. 34: The surface waviness on a copper block treated by electropolishing for 8 minutes without agitation. Picture was taken by a scanning electron microscope.

5. ENGINEERING DESIGN AND ALIGNMENT ISSUES

In practice an accelerating structure can not be fabricated from a single piece of metal. For the simplest case a structure is made from two identical pieces as depicted below:

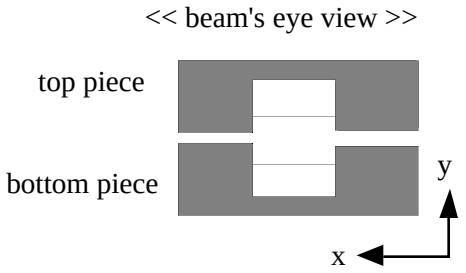

The schematic sketch for one half of a muffin-tin structure is depicted in Fig. 35.

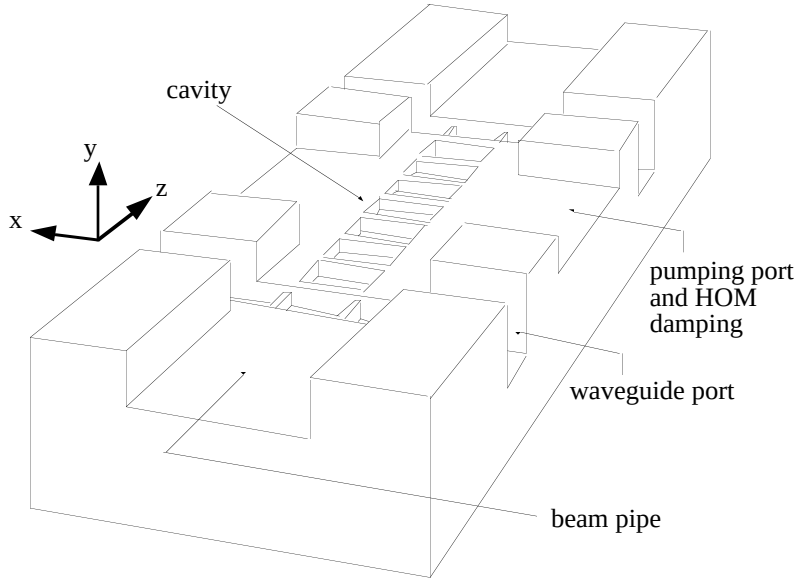

Fig. 35: The schematic sketch for one half of a muffin-tin structure with symmetrical ports for input and output waveguides.

When two pieces are assembled together and bonded, there is always some misalignment in x, y and z directions. An exaggerated sketch for misalignment in x direction is depicted below:

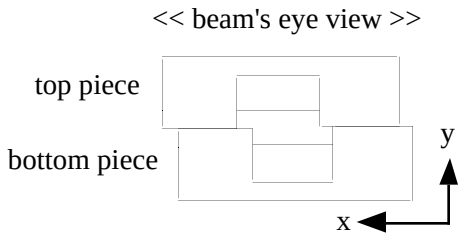

The alignment tolerances required for mm-wave accelerating structures are the same order of magnitude as the dimensional tolerances, i.e. 1 μm or less. One possible solution is to take advantage of the accuracy provided by fabrication technologies (e.g. LIGA can hold 2 μm tolerances or better) and machined a V-shaped gauge groove for structure assembling as depicted below:

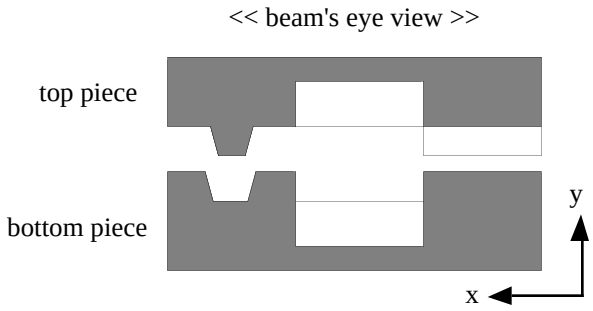

The width of the groove should be slightly larger than the one of the vane by 2-3 μm. This will set an upper limit for misalignments. The top and bottom pieces of the muffin-tin structure, with V-shaped vanes and grooves, are depicted in Figs. 36 and 37. The advantage of using V-shaped gauge grooves is that it is possible to achieve precise alignments in all directions simultaneously. As depicted in Fig. 36, this approach requires the design to have multiple level heights. A multi-level design is a challenge to micromachining techniques such as LIGA. Although microstructures with two level heights fabricated by LIGA have been reported recently[36], it is still uncertain whether the level height can be controlled within an accuracy of one micron or less. There are other alignment techniques being investigated. Alignment tolerances of ± 5 μm in translational direction of beam aperture by using anodic bonding has been reported[29]. Diffusion bonding is being considered as the choice of bonding structural components. The prerequisite for diffusion bonding is to have good surface finishes on all contact planes. This also manifests the importance of surface studies besides the concerns on field emission and RF breakdown.

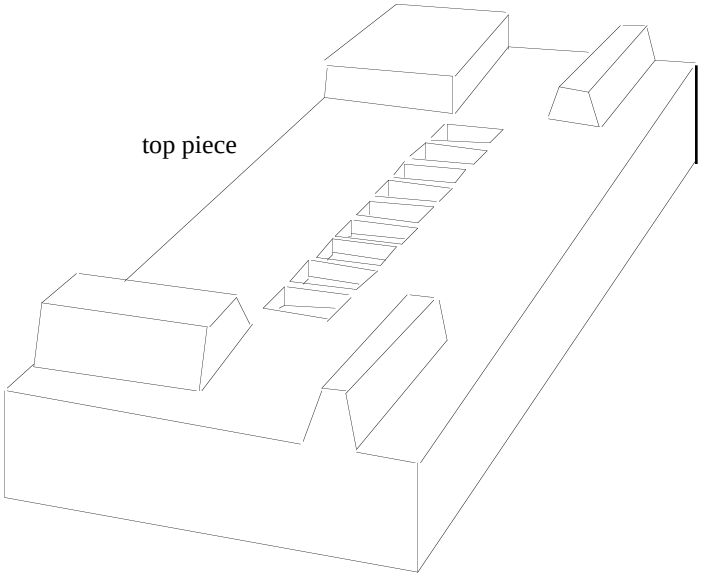

Fig. 36: The top piece of half of a muffin-tin structure with V-shaped vanes.

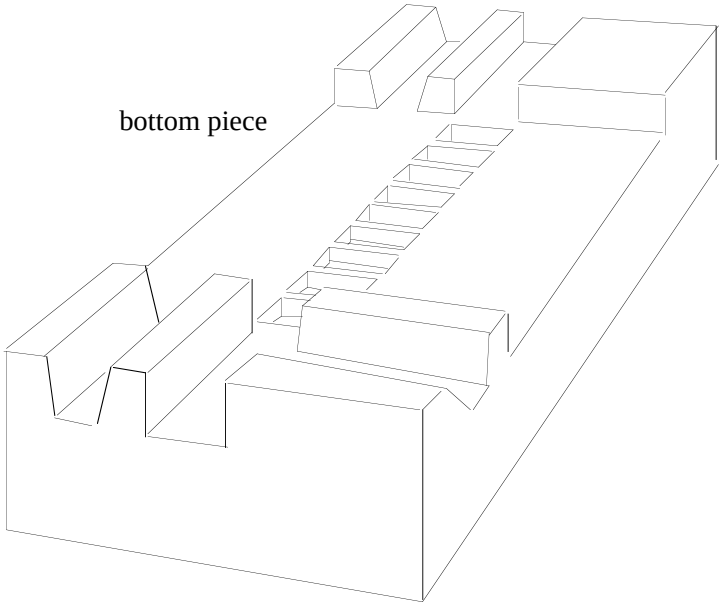

Fig. 37: The bottom piece of half of a muffin-tin structure with V-shaped grooves.

6. SUMMARY

Several fabrication techniques have been surveyed and discussed. The decision on the final choice of design and fabrication technique is quite involved. It will require a good understanding on the relationship between pulse heating and surface damage, properties of transverse wakefield, suppression of field emission and multipactor effects. The fabrication of mm-wave accelerating structures is testing the limit of conventional paradigm for accelerator design based on microwave technology.

ACKNOWLEDGMENTS

The authors would like to thank Eric Lundahl for performing coordinate measurements on test samples and Wayne Shen for helpful discussions.

REFERENCES

1. R.B. Palmer, in *AIP Conference Proceedings No.337, Montauk, NY 1994,* edited by R.C. Fernow (AIP Press, New York, 1995), pp.1- 15.

2. R.B. Neal et al. (eds.), *The Stanford Two-Mile Accelerator* (Benjamin, New York, 1968), p.96.

3. NLC design group, *Zeroth-Order Design Report for the Next Linear Collider,* SLAC Report 474.

4. H. Henke et al., Argonne National Laboratory Internal Report ANL/APS/MMW-1 (1993).

5. D.J. Whitehouse, *Handbook of Surface Metrology* (IOP Publishing, London, 1994).

6. I. Wilson in *RF Engineering for Particle Accelerators,* CERN 92-03 (1992), p.375.

7. R.H. Siemann (SLAC), private notes.

8. G. Bowden, NLC-ME-Note No. 8-96 (SLAC).

9. Y. Higashi (KEK), private communication.

10. This is performed with a dynamic focus optical scanner which is manufactured by UBM Corp., 544 Weddell Dr., Suite 1, Sunnyvale, CA 94089, U.S.A.

11. Fotofabrication Corp., 3758 Belmont Ave., Chicago, IL 60618, U.S.A.

12. Vaga Industries, http://www.bayrep.com/vaga.

13. Nat Wood, *CNC West* (August/ September 1993), p.16.

14. Ron Witherspoon Inc., 430 Industrial St., Campbell, CA 95008, U.S.A.

15. C.M. Rodia in *Metal Finishing Guidebook and Directory Issue,* edited by M. Murphy et al. (Elsevier Science, New York, 1995), p. 369.

16. C.A. Harper (ed.), *Handbook of Materials and Processes for Electronics* (McGraw-Hill, New York, 1970), p. 10-1.

17. A.J. Tuck Company, P.O. Box 215, 32 Tuck Rd., Brookfield, CT 06804.
18. S.M. Sze, *Semiconductor Devices: Physics and Technology* (Wiley, New York, 1985).

19. B. Loechel et al., *J. Vac. Sci. Technol.* **B13**, 2934 (1995).

20. B. Löchel et al., *Sensors Actuators* **A46**, 98 (1995).

21. P. Van Zant, *Microchip Fabrication,* 2nd ed. (McGraw-Hill, New York, 1995).

22. Ion Beam Milling, Inc., 1000 E. Industrial Park Dr., Manchester, N.H. 03103.

23. John Shott (Stanford University), private communication.

24. H. Mader in *Micro System Technologies 90,* edited by H. Reichl, (Springer-Verlag, Berlin, 1990), pp. 357- 365.

25. D. Bollinger et al., *Solid State Technol*. **27**, No.5 (May 1984), p. 111.

26. D. Bollinger et al., *Solid State Technol*. **27**, No. 6 (June 1984), p. 167.

27. I.W. Rangelow and H. Löschner, *J. Vac. Sci. Technol.* **B13**, 2394 (1995).

28. MicroScape, http://www.microscape1.com.

29. T.L. Willke and A.D. Feinerman, *J. Vac. Sci. Technol.* **B14**, 2524 (1996).

30. W. Ehrfeld in *Micro System Technologies 90,* edited by H. Reichl, (Springer-Verlag, Berlin, 1990), pp. 521- 537.

31. K.H. Jackson (Lawrence Berkeley National Laboratory), private communication.

32. J.F. Jumer in *Metal Finishing Guidebook and Directory Issue,* edited by M. Murphy et al. (Elsevier Science, New York, 1995), p. 420.

33. R.D. Cormia et al., "Electropolishing of Stainless Steel" presented at the *PCMI Annual Meeting*, Anaheim, CA, 1990 (Photo Chemical Machining Institute, Lafayette Hill, PA).

34. H. Diepers et al., *IEEE Trans. Nucl. Sci. Vol.* **20**, No. 3, 68 (1973).

35. E. Hoyt (SLAC), private communication.

36. J. Mohr in *Biomedical Applications of Synchrotron Radiation*, edited by E. Burattini et al. (IOS Press, Oxford, 1996), p. 181.